Biomaterials 33 (2012) 8003–8016

Contents lists available at SciVerse ScienceDirect

Biomaterials

journal homepage: www.elsevier.com/locate/biomaterials

Corneal repair by human corneal keratocyte-reprogrammed iPSCs and amphiphatic carboxymethyl-hexanoyl chitosan hydrogel

Yueh Chien [a,b,i,1], Yi-Wen Liao [a,1], Dean-Mo Liu [d], Heng-Liang Lin [a,b], Shih-Jen Chen [c,h], Hen-Li Chen [a], Chi-Hsien Peng [c,e], Chang-Min Liang [f,**], Chung-Yuan Mou [g], Shih-Hwa Chiou [a,b,c,h,i,*]

[a] Institute of Oral Biology, National Yang-Ming University, Taipei, Taiwan, ROC
[b] Institute of Pharmacology, National Yang-Ming University, Taipei, Taiwan, ROC
[c] Institute of Clinical Medicine, National Yang-Ming University, Taipei, Taiwan, ROC
[d] Department of Materials Science and Engineering, National Chiao Tung University, Hsinchu, Taiwan, ROC
[e] Department of Ophthalmology, Shin Kong Wu Ho-Su Memorial Hospital & Fu-Jen Catholic University, Taipei, Taiwan, ROC
[f] Department of Ophthalmology, Tri-service General Hospital & National Defense Medical Center, Taipei, Taiwan, ROC
[g] Department of Chemistry, College of Science, National Taiwan University, Taipei, Taiwan, ROC
[h] Department of Ophthalmology, Taipei Veterans General Hospital, Taipei, Taiwan, ROC
[i] Department of Medical Research and Education, Taipei Veterans General Hospital, Taipei, Taiwan, ROC

ARTICLE INFO

Article history:
Received 5 May 2012
Accepted 15 July 2012
Available online 31 July 2012

Keywords:
Cornea
Wound healing
Hydrogel
Stem cell
Chitin/chitosan

ABSTRACT

Induced pluripotent stem cells (iPSCs) have promising potential in regenerative medicine, but whether iPSCs can promote corneal reconstruction remains undetermined. In this study, we successfully reprogrammed human corneal keratocytes into iPSCs. To prevent feeder cell contamination, these iPSCs were cultured onto a serum- and feeder-free system in which they remained stable through 30 passages and showed ESC-like pluripotent property. To investigate the availability of iPSCs as bioengineered substitutes in corneal repair, we developed a thermo-gelling injectable amphiphatic carboxymethyl-hexanoyl chitosan (CHC) nanoscale hydrogel and found that such gel increased the viability and CD44 + proportion of iPSCs, and maintained their stem-cell like gene expression, in the presence of culture media. Combined treatment of iPSC with CHC hydrogel (iPSC/CHC hydrogel) facilitated wound healing in surgical abrasion-injured corneas. In severe corneal damage induced by alkaline, iPSC/CHC hydrogel enhanced corneal reconstruction by downregulating oxidative stress and recruiting endogenous epithelial cells to restore corneal epithelial thickness. Therefore, we demonstrated that these human keratocyte-reprogrammed iPSCs, when combined with CHC hydrogel, can be used as a rapid delivery system to efficiently enhance corneal wound healing. In addition, iPSCs reprogrammed from corneal surgical residues may serve as an alternative cell source for personalized therapies for human corneal damage.

1. Introduction

The cornea is a transparent, avascular tissue on the ocular surface of the eye, and its integrity is vital to normal vision [1–3]. The covered stratified epithelium is responsible for maintaining the integrity and smooth surface of the cornea as well as providing a barrier against environmental stress [2,3]. Stem cells from limbal regions exhibit the ability to replace and regenerate corneal epithelium cells, which participate in the dynamic equilibrium of the corneal surface [2–5]. Severe damage to limbal stem cells (LSCs) usually manifests as vascularization and chronic inflammation of the cornea, ingrowth of fibrous tissue, and corneal opacification [4,5]. LSCs possess the potential for self-renewal and multi-directional differentiation, and the use of amniotic membrane-based transplantation (AMT) with cultured LSCs has become an effective treatment for regenerating epithelial cells on the corneal surface [6]. However, the AMT cultivation methods for corneal epithelial tissues currently used in clinical transplantation applications require long periods of time. In addition, it is still

* Corresponding author. Department of Ophthalmology, Department of Medical Research and Education, Taipei Veterans General Hospital; No. 201, Sec. 2, Shih-Pai Road, Taipei 11217, Taiwan, ROC.
** Corresponding author. Department of Ophthalmology, Tri-service General Hospital & National Defense Medical Center, No. 325, Sec.2, Chenggong Road, Neihu District, Taipei 114, Taiwan, ROC.
E-mail addresses: doc30875@ndmctsgh.edu.tw (C.-M. Liang), shchiou@vghtpe.gov.tw (S.-H. Chiou).
[1] These authors contributed equally to this work (co-first).

0142-9612/$ – see front matter © 2012 Elsevier Ltd. All rights reserved.
http://dx.doi.org/10.1016/j.biomaterials.2012.07.029

unclear if using donor-provided amniotic membranes increases the chances of AMT-related infection, inflammation, or other biosafety risks [7–9].

Induced pluripotent stem cells (iPSCs) provide a unique platform that can be applied to investigations of disease mechanisms, drug discovery and personalized treatments [10]. The accumulated research on this topic has demonstrated that human iPSCs can be generated from human adult cells via transfection with the transcription factors Oct3/4, Sox2, Klf4, and c-Myc [11–13]. These reprogramming technologies have shown great potential for use in the modeling and treatment of human diseases, without associated ethical or immunorejection issues [10]. Remarkable efforts have been made to evaluate the efficacy of iPSC treatments in various disease models, including fulminant hepatic failure, acute lung injury, and ischemic stroke [14–16]. Recently, iPSCs generated from swine fetal fibroblasts were demonstrated to possess the ability to differentiate into photoreceptors in vitro and were able to integrate into a damaged neural retina [17]. Notably, a recent human embryonic stem cell (ESC) trial addressing macular degeneration showed that transplantation of ESC-derived retinal pigment epithelium cells (RPEs) could improve a patient's visual acuity without resulting in hyperproliferation or increased tumorigenicity [18]. However, it is still unknown whether human ESCs or iPSCs have the potential to rescue corneal dysfunction through corneal differentiation or cytoprotection. Therefore, it will be useful to investigate the therapeutic utility of iPSC transplantation with respect to corneal injury and reconstruction.

In the present study, we attempted to investigate whether human corneal fibroblasts (keratocytes) could be reprogrammed into human iPSCs showing pluripotent properties. To prevent feed cell contamination and improve the clinical utility of these reprogrammed iPSCs, we have developed a feeder-free (without mouse embryonic fibroblast (MEF) feeder cells) and serum-free method to stably expand human iPSCs in vitro. To improve iPSC delivery and engraftment, a thermo-gelling injectable carboxymethyl-hexanoyl chitosan (CHC) nanogel was developed that contains self-assembled nanocapsules of amphiphilically modified chitosan. Subsequently, we evaluated whether the viability and pluripotent properties of human corneal keratocyte-derived iPSCs can be retained in a CHC hydrogel system, and explored the therapeutic potential of keratocyte-derived iPSCs using CHC hydrogel as delivery vehicle on corneal impairment, in models of corneal damage induced by either chemical burns or surgical ablation. Our findings may provide an alternative therapeutic strategy for treating corneal injury induced by mechanical or chemical insults.

2. Materials and methods

2.1. Human iPSC generation and culture

This research followed the tenets of the Declaration of Helsinki, and all samples were obtained after patients had given informed consent. iPSCs were reprogrammed via the transduction of pMXs vectors encoding the transcription factors Oct-4, Sox2, Klf4, and c-Myc. The Plat-A cells used for plasmid transfection were incubated overnight at a density of 2.5×10^6 cells per 100-mm dish. The next day, 10 μg of pMXs-containing cDNA was transfected into the Plat-A cells with 10 ml of fresh DMEM using TransIT®-LT1 (Mirus, Madison, WI). At 48 h after transfection, virus-containing medium was collected for target cell infection. In preparation for viral infection, 5×10^4 target cells were seeded per well into 6-well plates one day prior to transduction. Supernatants containing equal amounts of each of the four retroviruses were filtered through a 0.45 μm filter and supplemented with 10 μg/ml polybrene (Sigma), and the medium in the 6-well plates was replaced with the virus-containing medium. The 6-well plates were centrifuged at 2250 rpm for 1 h, and the medium was then replaced. At day 7 post-infection, target cells were passaged onto mitotically inactivated MEF feeder layers and cultured using human ESC medium. The drugs SB431542 (2 μM, Stemgent), PD0325901 (0.5 μM, Stemgent), and thiazovivin (0.5 μM) were added to the culture medium to aid in colony formation [19]. Drug-containing medium was replaced daily until iPSC colonies were detected. Undifferentiated iPSCs were maintained on mitotically inactivated MEFs (50,000 cells/cm^2) in human ESC medium (DMEM/F12 (Gibco) supplemented with 20% KnockOut serum replacer (KSR; Invitrogen), 0.1 mM non-essential amino acids (Invitrogen), 1 mM ι-glutamine, 0.1 mM ß-mercaptoethanol, 10 ng/ml recombinant human basic fibroblast growth factor (bFGF), and antibiotics (Gibco). To prevent the mouse embryonic fibroblasts (MEF) contamination, human iPSCs or human ESC cells were transferred to feeder-free/serum free culture system in CSTI-8 medium (Cell Science & Technology Institute Inc.) without KSR supplementation. Briefly, the 100 mm Petri dish was coated by fibronectin (F1141, Sigma). iPSCs were dissociated with 2 U/ml dispase (Invitrogen) and then added into precoated dish with CSTI-8 medium (Cell Science & Technology Institute Inc, Tokyo, Japan) without KSR supplementation. These characteristics of the human iPSCs cultured using the serum-free/feeder-free system were comparable to the characteristics of iPSCs cultured using the conventional MEF feeder system.

2.2. Bisulfite sequencing

Bisulfite reaction was performed using the Imprint DNA Modification Kit (Sigma) according to the manufacturer's instruction. 500 ng of genomic DNA were used for each one-step modification reaction. Post-modified DNA was cleaned up and amplified by PCR using primers as described previously [20,21]. PCR products were cloned into pGEM-T Easy vector (Promega), and 10 randomly selected clones for each sample were sequenced.

2.3. Digital ratio imaging for intracellular calcium

The intracellular calcium ratio imaging was measured as described previously [16]. Differentiated cells were treated with 5 lM Fura-2 AM in the loading buffer for 30 min at 37 °C. The coverslips were washed three times in the loading buffer and then mounted in a recording chamber on the platform of an inverted epifluorescence microscope. Cells were stimulated with high K+ buffer (150 mM) at indicated conditions. When measuring {Ca2+}i using ratio imaging method as described above, micropipette with a tip of 2 lm diameter opening was used for delivery of very small amount (picoliter to nanoliter) of reagents locally by a 15 psi ejection pulse for 0.5 s (Picospritzer II, General Valve, USA). The acquisition of {Ca2+}i ratio image with excitations of 340 and 380 nm was collected every 0.5 s by an imaging system using a high speed cooled CCD camera (Micro-MAX: 782YHS, Princeton Instruments, Roper Scientific, Trenton, NJ, USA) and a xenon lamp within a monochromator as a excitation light source (Polychrome II, T.I.L.L. Photonics, Germany), and a software Axon Image Workbench 2.0 (Axon Instruments, Foster city, CA, USA).

2.4. MTT assay

For evaluation of cell survival, cells were seeded on 24-well plates at a density of 2×10^4 cells/well, followed by the addition of methyl thiazol tetrazolium (MTT; Sigma) at the end of cell culture. The amount of MTT formazan product was determined using a microplate reader at an absorbance of 560 nm (SpectraMax 250, Molecular Devices, Sunnyvale, CA, USA).

2.5. Real-time reverse transcription-polymerase chain reaction (RT-PCR)

Real-time RT-PCR was performed as previously described [22]. For real-time RT-PCR analysis, the total RNA of cells was extracted by using the RNAeasy kit (Qiagen, Valencia, CA). Briefly, the total RNA (1 mg) of each sample was reversely transcribed in 20 mL using 0.5 mg of oligo dT and 200 U Superscript II RT (Invitrogen, Carlsbad, CA). The amplification was carried out in a total volume of 20 ml containing 0.5 mM of each primer, 4 mM MgCl2, 2 ml LightCycler FastStart DNA Master SYBR green I (Roche Diagnostics, Pleasanton, CA) and 2 ml of 1:10 diluted cDNA. The quantification of the unknown samples was performed by LightCycler Relative Quantification Software, version 3.3 (Roche Diagnostics). In each experiment, the GAPDH housekeeping gene was amplified as a reference standard. PCR reactions were prepared in duplicate and heated to 95uC for 10 min followed by 40 cycles of denaturation at 95uC for 10 s, annealing at 55uC for 5 s, and extension at 72uC for 20 s. All PCR reactions were performed in duplicate. Standard curves (cycle threshold values versus template concentration) were prepared for each target gene and for the endogenous reference (GAPDH) in each sample. The primers and cycling conditions for RT-PCR are shown as Table 1.

2.6. Preparation of CHC thermo-gelling solutions

Carboxymethyl-hexanoyl Chitosan (CHC) was purchased from Advance Delivery Technology Inc., Hsinchu, Taiwan. Amphiphatic carboxymethyl-hexanoyl chitosan hydrogel was synthesized and characterized as described previously [23]. Glycerol was purchased from Sigma–Aldrich. β-glycerol phosphate disodium salt hydrate (β-GP) was from Merck. The CHC polymer powder was dissolved in distilled water and freeze-dried to form sponge-like powder for a subsequent dissolution in selective medium. 0.6 g of CHC sponge-like powder was added in 20 ml medium under stirring on ice bath, until the powder totally dissolved in the medium to form a viscous solution. After then, 50 μg β-GP was dissolved in 1 ml of the CHC/medium solution under stirring on ice. The final solution with thermally induced sol–gel

Table 1
The sequences for the primers of RT-PCR.

Gene name	Primer sequence	Product length
Klf4	Sense: CCGCTCCATTACCAAGAGCT Antisense: ATCGTCTTCCCCTCTTTGGC	76 bp
Nanog	Sense: ATTCAGGACAGCCCTGATTCTTC Antisense: TTTTTGCGACACTCTTCTCTGC	76 bp
Oct4	Sense: GTGGAGAGCAACTCCGATG Antisense: TGCTCCAGCTTCTCCTTCTC	86 bp
Sox2	Sense: CGAGTGGAAACTTTTGTCGGA Antisense: TGTGCAGCGCTCGCAG	74 bp
GAPDH	Sense: CTCATGACCACAGTCCATGC Antisense: TTCAGCTCTGGGATGACCTT	155 bp

Abbreviation: GAPDH, glyceraldehyde-3-phosphate dehydrogenase.

transition was observed when the temperature increased from 4 °C and formed a solid gel at temperature greater than 37 °C.

2.7. In vivo alkali burn-injured rat model

The rat cornea alkali burn model was implemented as previously described, with slight modifications [24]. Briefly, rats were anaesthetized via peritoneal administration of chloral hydrate (300 mg/kg). Clean filter paper cut with a trephine of 2 mm in diameter was placed on the central cornea, and 2 μL of 0.15 M NaOH was applied to the right cornea of each mouse for 1 min following the application of topical alkaline to each eye. The corneal and limbal epithelial cells were removed with a No. 15 knife and rinsed with normal saline. The injured eyes of each mouse were covered with either CHC hydrogel alone or CHC hydrogel seeded with iPSCs at a density of 2×10^4 cells/20 ml after closing the eyelid with a 6-0 silk suture. The ocular condition and morphology were observed and photographed on post-treatment days 1, 3, 5, and 7. At each stage, the area of the corneal epithelial defect was monitored using fluorescent staining paper. In vivo GFP imaging was performed using an illuminating device (LT-9500 Illumatool TLS equipped with an excitation illuminating source {470 nm} and filter plate {515 nm}. The results were subsequently analyzed using Image Pro-plus software [14].

2.8. Statistical analysis

The results are expressed as mean ± SD. Statistical analyses were performed using the *t*-test for comparing two groups, and one-way or two-way ANOVA, followed by Bonferroni's test, was used to detect differences among three or more groups. Results were considered statistically significant at $P < 0.05$.

3. Results

3.1. Characterization of human keratocyte-derived iPSCs

The isolation and cultivation of corneal stem cells has been reported previously. However, the question of whether corneal cells or keratocytes can provide alternative cell sources to be reprogrammed into iPSCs remains to be determined. In the present study, we isolated human corneal keratocytes and reprogrammed these cells into iPSCs via transfection with retroviral vectors encoding the transcription factors Oct4, Sox2, Klf4, and c-Myc. Briefly, human corneal keratocytes (Fig. 1A; upper panel) were isolated from donor corneal tissues obtained from surgical residues (the residual tissues of donor cornea for the transplanted graft of penetrating keratoplasty). The cultivated corneal keratocytes presented a fibroblast-like shape (Fig. 1A; upper panel), and were then transfected with four genes (Oct4/Sox2/Klf4/c-Myc) using lentiviral vectors. Seven days after viral transfection, the cells were passaged onto mitotically inactivated MEFs (Fig. 1A; middle panel) and cultured with embryonic stem cell (ESC) media containing SB431542, PD0325901, and thiazovivin, which facilitates iPSC colony formation as described previously [19]. As the reprogramming progressed, these cells gradually formed colonies of increasing size (Fig. 1A; lower panels). These colonies were cultivated on the MEF feeder cells in KSR-based media and stained positive for alkaline phosphate (ALP) and exhibited a morphology indistinguishable from that of human ESCs (Fig. 1B; Suppl. materials and methods). To improve the potential of clinical utility and prevent the mouse fibroblast contamination, the human keratocyte-reprogrammed iPSCs (KC-iPSCs) were transferred to feeder-free culture in CSTI-8 medium without KSR supplementation and further stably passaged to at least 30 passages (Fig. 1C). These 30th KC-iPSCs showed strong positivity of ALP and the chromosomal analysis showed identical pattern with parental keratocytes with normal karyotyping (Fig. 1C). Bisulfite sequencing showed that the Oct4 and Nanog promoters in the 30th KC-iPSCs exhibited much lower methylation state than parental keratocytes (Fig. 1D). Using microarray analysis, we next compared the gene expression profile among keratocyte, keratocyte-reprogrammed iPSCs (KC-iPSC), and human ESCs (hESCs). The profiles of the differentially-expressed genes based on their functions in the Gene Ontology database were displayed in Fig. 1E and Suppl. Fig. 1A. Remarkably, gene expression within the subset of 10th, 20th, and 30th KC-iPSCs resembled the expression patterns of human ESC H9 line at different passages (10th, 20th, and 30th passages), but not keratocytes (Fig. 1E). RT-PCR results showed that 30th KC-iPSCs expressed the genes Oct4, Sox2, Nanog, REX, and DPPA2, which are also expressed in the human ESCs (Fig. 1F). Immunofluorescence results indicated that the iPSCs from the 30th passage of these iPSC colonies showed strong expression of Oct4, Nanog, SSEA4, and Tra-1-60 (Fig. 1G). Importantly, these characteristics of the human iPSCs cultured using the serum-free/feeder-free system were comparable to the characteristics of iPSCs cultured using the conventional MEF feeder system (Data not shown). Thus, our data demonstrated that human iPSC cell lines can be reprogrammed from adult corneal tissues and that these human keratocyte-reprogrammed iPSCs present ESC-like properties and can be greatly expanded in vitro.

The genomic traits of human fibroblast, keratocyte, keratocyte-reprogrammed iPSCs (KC-iPSCs), and human ESCs (hESCs) were further examined using gene expression microarray analysis. Multi-dimensional scaling (MDS) and average distance analysis further showed that the gene expression pattern of 30th KC-iPSCs was closer to the gene signature of hESCs, but was dissimilar to the human fibroblast and the parental keratocytes (Fig. 2A and Suppl. Fig. 1B). 30th KC-iPSCs showed the strong positivity of ALP (Fig. 2B, left and middle), and 30th KC-iPSC-derived embryoid bodies (EBs) could be further differentiated into osteocyte-like cells and adipocyte-like cells, as confirmed by alizarin red and oil red O staining, respectively (Fig. 2B, right). Using differentiation protocols for tridermal lineages, the 30th KC-iPSCs-derived EBs could also be induced to differentiate into neuron-like cells, smooth muscle cells and hepatocyte-like cells (ectoderm, mesoderm, and endoderm). Immunofluorescence analysis demonstrated that the expression of markers specific to each lineage, i.e., nestin, SMA, and AFP, respectively, was similar to the levels of expression found in the H9 ESC line (Fig. 2C). To further determine the properties of the voltage-dependent calcium channels in iPSC-derived neuron-like cells (Fig. 2D), the change ratio of intracellular calcium concentrations was monitored using a digital calcium imaging assay with a Fura-2 fluorescence system. The ratio of fura340 fluorescence significantly increased in response to the addition of high concentrations of potassium (150 mM), indicating a rapid influx of intracellular calcium as the property of neuronal cells (Fig. 2E and F). Taken together, our data demonstrated that these human keratocyte-reprogrammed iPSCs were capable of multi-lineage differentiation, with the resultant cells showing functional characteristics after the application of stepwise protocols.

3.2. Preparation of CHC nanoscale hydrogels

We next sought to prepare carboxymethyl-hexanoyl chitosan (CHC) hydrogels and examine whether the iPSCs remained viable and retained their stemness properties in the CHC hydrogels.

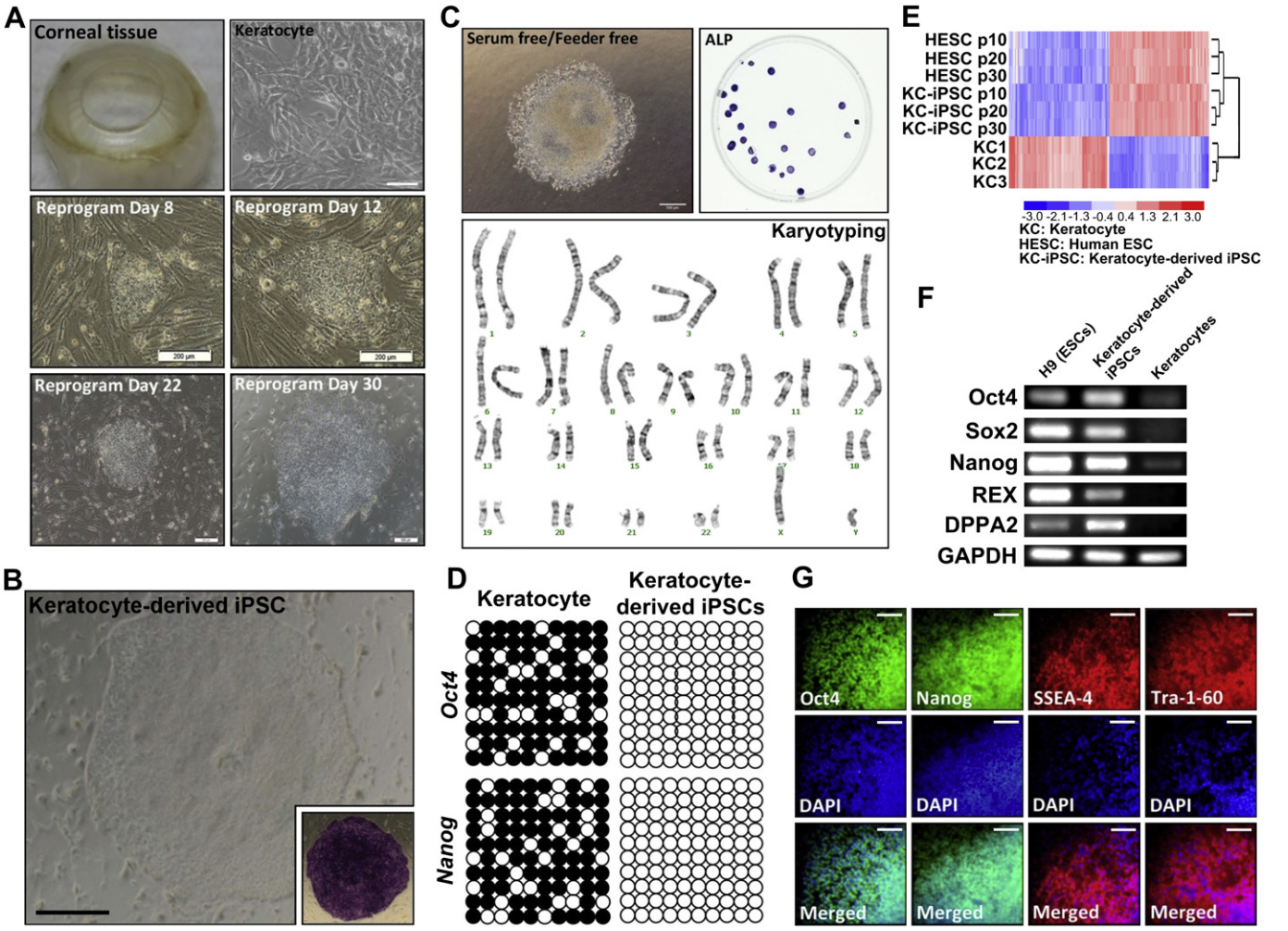

Fig. 1. Characterization of human corneal keratocyte-reprogrammed iPSCs. (A) Isolation of corneal keratocytes from surgical residues of donor corneal tissue. The cultivated corneal keratocytes presented fibroblast-like morphologies (upper right). After transfected with Oct4/Sox2/Klf4/c-Myc and cultured on MEFs as a feeder, the morphology of reprogramming keratocytes was changed to small size and compact colony in reprogram day 8 and 12 (middle panel). The mature colonies of keratocyte-reprogrammed iPSCs were formed at reprogram day 30 (lower panel). Scale bar = 200 μm; (B) The keratocyte-reprogrammed iPSCs (KC-iPSCs) were stably passaged on MEFs feeder and stained positive for alkaline phosphatase (ALP). Scale bar = 200 μm; (C) Under this serum-free and MEF feeder-free culture system, these KC-iPSCs can be stably cultured through at least 30 passages (upper left) and retain both high ALP activity (upper right) and showed the normal karotyping (lower panel). Passage number does not affect the ability of iPSCs to form colonies. (D) Bisulfite sequencing comparing the methylation status of Oct4 and Nanog promoters in 30th KC-iPSCs and parental keratocytes. (E) Microarray analysis and (F) RT-PCR results indicating an ESC-like gene expression pattern in keratocyte-reprogrammed iPSCs, including 10th (p10), 20th (p20), 30th (p30) KC-iPSCs. (G) The immunofluorescence assay showed that colonies of iPSCs express Oct4, Nanog, SSEA1, SSEA4, and Tra-1-60. DAPI: nuclear staining. Scale bar = 100 μm.

Briefly, thermosensitive CHC hydrogels were prepared as depicted in Fig. 3A and as described in the Materials and Methods. Fig. 3B presents the concept underlying CHC nanogel preparation. Disodium glycerophosphate (β-GP) was used to neutralize the positive charge on the CHC nanocapsules and reduce the repulsive forces that arise between CHC nanocapsules at elevated temperatures, which gave rise to a sol–gel transition with increased temperatures. The ampiphilic CHC self-assembled into nanocapsules in an aqueous environment. In acidic to neutral pH ranges, the nanocapsules carried positive charges on their shell, derived from the protonation of amino groups. Glycerol was added to achieve additional hydrogen bonding between CHC nanocapsules, glycerol and water, which could influence gelation behavior as well as improve gel strength. The structural formula of the CHC hydrogels is depicted in Fig. 3C. To determine the nanostructure of the CHC gels, formed gels (C3-β5-G10) were dried and analyzed using transmission electron microscopy. The microscopy indicated that the CHC polymer had indeed self-assembled into nanocapsules in solution when the surrounding temperature increased, a CHC gel was formed through the aggregation or coagulation of the CHC nanocapsules into a continuous network. Similar to a previous report [25], the diameters of the nanocapsules were approximately 50–100 nm, which provided an excellent scaffold for iPSC intercalation in the following experiments (Fig. 3D). Fig. 3E shows that the gelation temperature of this CHC nanoscale hydrogel is at 37 °C, making this chemical compound an ideal carrier for cell transplantation under ambient body temperatures.

3.3. iPSC fate in CHC nanoscale hydrogels

To ensure the viability of the iPSCs after implantation into the CHC nanoscale hydrogels, we investigated the cell survival rate and mRNA expression of stemness genes in iPSCs embedded in CHC hydrogels, both with and without culture media. To effectively monitor the fate of the embedded iPSCs within the CHC hydrogels, the keratocyte-reprogrammed iPSCs were co-transfected with

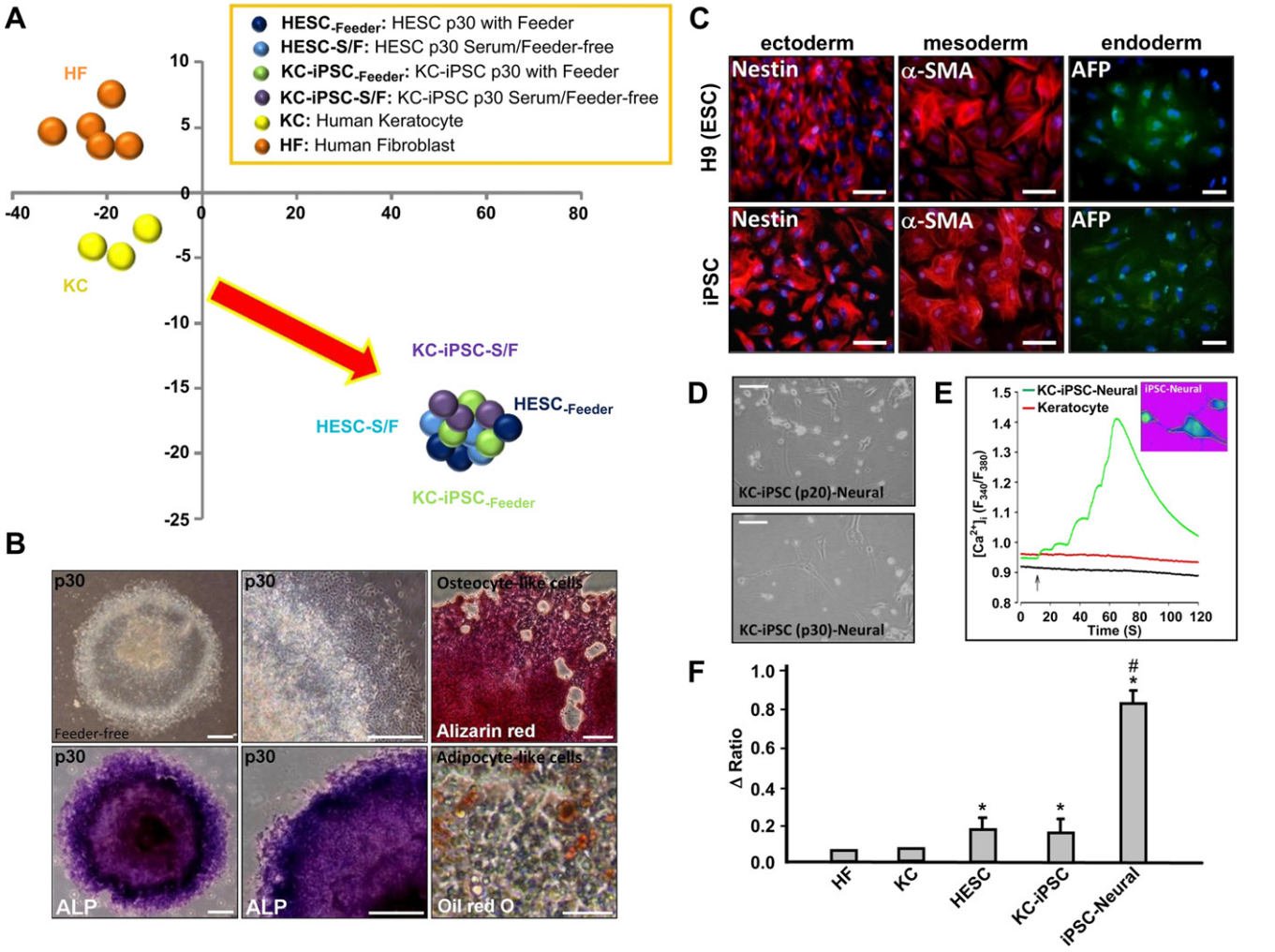

Fig. 2. The pluripotent differentiation potential of human corneal keratocyte-reprogrammed iPSCs under serum- and feeder-free culture system. (A) Microarray with bioinformative analysis showed that the gene expression pattern of 30th keratocyte-reprogrammed iPSCs (KC-iPSCs) was more similar to that of human embryonic stem cell (HESC) but was dissimilar to the human fibroblasts (HF) and parental keratocytes (KC). (B) Left and middle: 30th KC-iPSCs presented the self-renewal ability to form the colonies and were strongly stained positive for alkaline phosphate (ALP), Scale bar = 200 μm; Right: differentiation of 30th KC-iPSCs into osteocyte-like cells (positive for Alazine red staining; upper right panel) and adipocyte-like cells (positive for oil red O staining; lower right panel), Scale bar = 50 μm. (C) Using differentiation protocols of tridermal lineages, iPSC-derived EBs were differentiated into neuron-like cells (ectoderm), smooth muscle cells (mesoderm), and hepatocyte-like cells (endoderm). Immunofluorescence results indicating the expression of specific markers of each lineage (nestin, SMA, and AFP, respectively). Scale bar = 200 μm. (D) Morphology of 20th and 30th keratocyte-reprogrammed iPSCs (KC-iPSCs). (E) Microscopy results showing the intracellular calcium fluctuation detected in HF, KC, KC-iPSCs and iPSC-derived neuron-like cells. In panel E, $^{*}P < 0.05$ vs. KC.

a vector encoding pCX-EGFP for constitutive expression of green fluorescence protein. MTT assays and GFP imaging both indicated that the iPSCs proliferated in the presence of culture media in the CHC hydrogel (Fig. 4A and B). As detected using quantitative RT-PCR, the expression of Oct4, Sox2, Nanog, and Klf4 was retained in CHC hydrogels containing media (Fig. 4C). It has been reported that CD44 is a receptor for hyaluronic acid and that interactions between hyaluronic acid and CD44 promote fibroblast adhesion and motility, thereby facilitating tissue repair and remodeling of injured sites [26]. Flow cytometry analysis of the CD44 surface marker indicated time-dependent elevation of the percentage of $CD44^{+}$ iPSCs in CHC hydrogel containing culture media for seven days (Fig. 4D and E). Collectively, the iPSCs exhibited a normal growth ability and constitutive expression of stemness genes in CHC hydrogel-containing culture media, indicating that the formulation of the CHC hydrogel and applied cultivation conditions created an excellent biocompatible niche for iPSC growth.

3.4. iPSCs and CHC hydrogels in ex vivo transplantations

Given that CHC nanoscale hydrogel (nanogel) possesses thermosensitive, rapid-gelling and injectable properties, it was critical to examine the bioavailability of the iPSC/CHC hydrogel mixture for ex vivo transplantation. We therefore investigated the fate of iPSCs embedded in CHC hydrogel in a rat model of in vivo corneal wound healing. As shown in Fig. 5A and B, the GFP-labeled keratocyte-reprogrammed iPSCs were trypsinized and then premixed with cold CHC hydrogel. Subsequently, this iPSC/CHC hydrogel mixture was gently applied to a corneal epithelial abrasion (Fig. 5B). After application of the iPSC/CHC hydrogel mixture to the corneal wound, a warm ambient temperature facilitated a sol-to-gel transition, which occurred within 10 min. In Fig. 5B, we present a further evaluation of the growth of these GFP-labeled keratocyte-reprogrammed iPSCs on ex vivo CHC-nanogel transplants. One day after transplantation, longitudinal sections of the eye indicated that the iPSC/CHC hydrogel mixture formed a smooth bio-scaffold layer

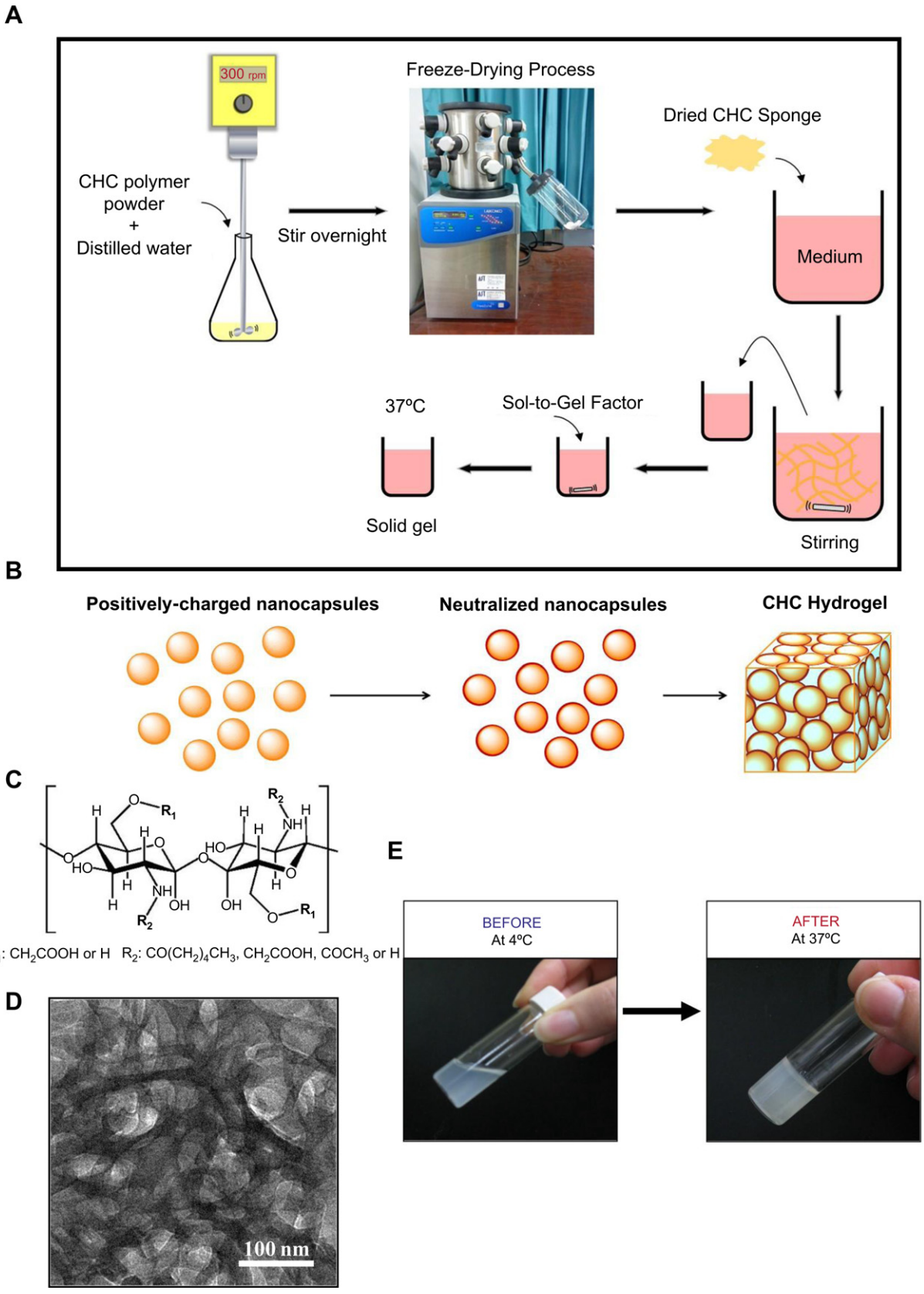

Fig. 3. CHC nanoscale hydrogel preparations. (A) Procedures for CHC nanoscale hydrogel preparation. (B) Nanocapsule structures formed by amphiphatic CHC hydrogel. (C) The structural formula of the CHC hydrogels. (D) Transmission electron microscopy results indicating the self-assembly of CHC hydrogels into nanocapsule microstructures at increased ambient temperature. (E) Thermosensitive sol-to-gel transition properties of the CHC hydrogel.

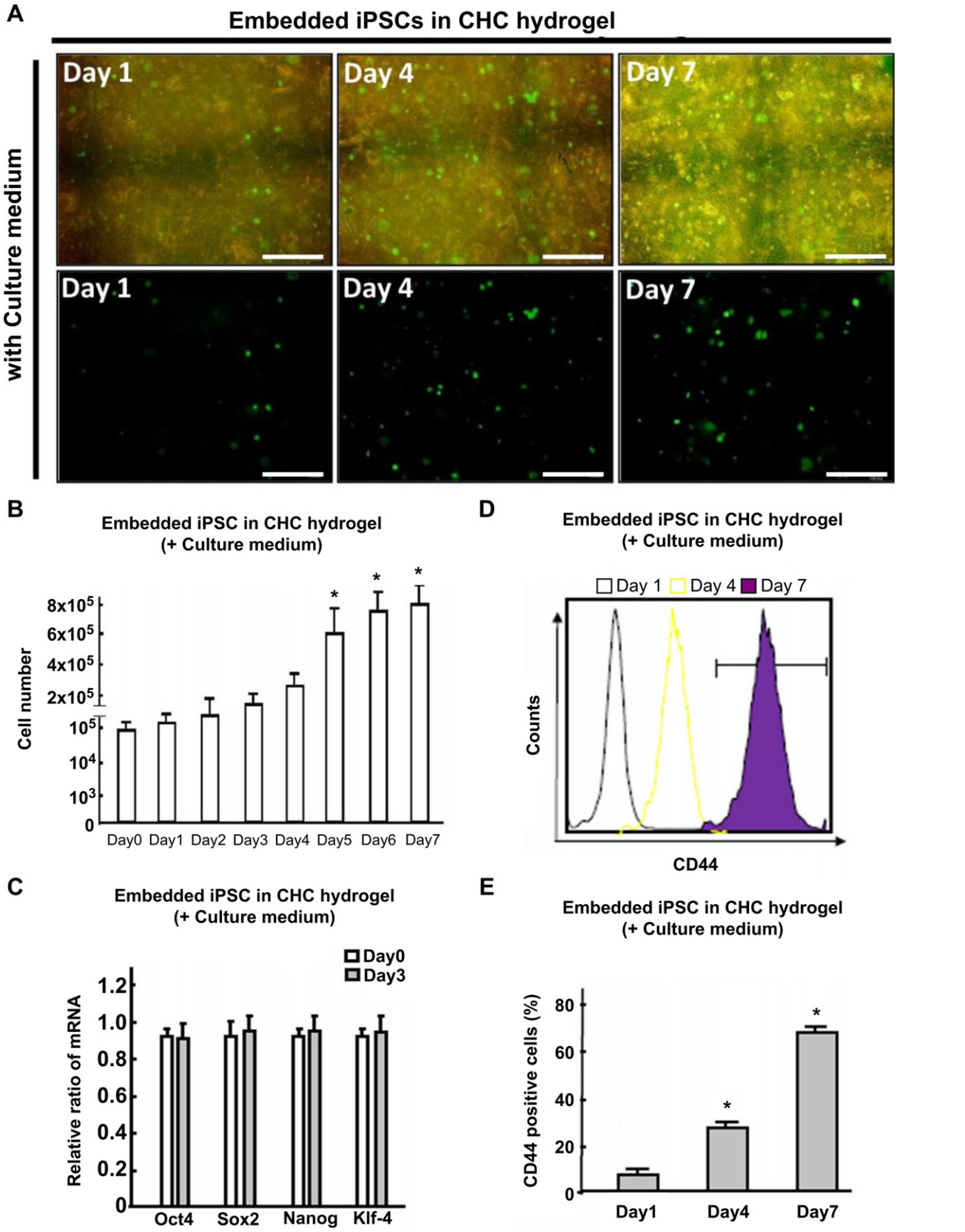

Fig. 4. Cell viability and ESC-like gene expression of iPSCs embedded in CHC hydrogel. (A) Human corneal keratocyte-reprogrammed iPSCs co-transfected with a vector encoding pCX-EGFP constitutively expressing green fluorescence protein. GFP-expressing iPSCs proliferating in the presence of culture media in the CHC hydrogel. Upper: bright field; lower: dark field. Scale bar = 100 μm (B) MTT assay showing the viability of keratocyte-reprogrammed iPSCs in the presence of culture medium. (C) Quantitative RT-PCR results indicating relative stem cell marker gene expression (for Oct4, Sox2, Nanog, and Klf4) in the presence of culture media. (D) Flow cytometry analysis indicating the percentage of $CD44^+$ iPSCs in CHC hydrogel-containing culture media throughout the culture period.

on the surface of the corneal wound in the epithelium abrasion model (Fig. 5C). Histological examination and H & E staining further showed the nanocapsule microstructure of the CHC hydrogel in which the iPSCs were intercalated (Fig. 5D). Notably, a positive DAPI signal indicated all viable cells co-localized with GFP-expressing iPSCs in the ex vivo CHC-nanogel transplant on the abrasion-injured cornea (Fig. 5C, middle and right). Taken together, these findings indicate that the use of the CHC hydrogel combined with culture media creates an ideal bioscaffold for iPSC intercalation and survival. Given the known tissue repair activity of iPSCs [14,15], this iPSC/CHC hydrogel mixture provides a source of cells and an alternative microenvironment that together promote corneal wound repair and tissue remodeling.

3.5. iPSC/CHC hydrogel enhanced corneal repair

We next attempted to investigate the therapeutic potential of the combination of the CHC nanoscale hydrogel and iPSCs with respect to wound healing following surgical (mechanical) abrasion-induced corneal damage. Corneal epithelium abrasion was carried out surgically (Fig. 6A), followed by the immediate application of either CHC nanoscale hydrogel (nanogel) alone or a mixture of CHC hydrogel and iPSCs. The corneal wound area was stained using fluorescent dye and quantified under UV-light illumination (Fig. 6A and B). Five days after surgical abrasion, the CHC hydrogel alone treatment slightly reduced the corneal wound area, and combined treatment of iPSC/CHC hydrogel further facilitated wound healing, compared to the control wound group (Fig. 6A and B). To assess the wound healing rate among all groups, we monitored the corneal wound repair in response to each treatment at different days after corneal epithelial abrasion. At post-abrasion day 3, the iPSC/CHC hydrogel combined treatment has shown a remarkable effect that reduced the corneal wound, and completely repaired the corneal epithelial wound at post-abrasion day 7 (Fig. 6C and D). Comparing with the combined treatment, CHC hydrogel alone also improved wound healing and led to the complete wound repair at post-abrasion day 9 (Fig. 6D). On the contrary, the completion of wound healing in control wound group was observed approximately at post-abrasion day 10 (Fig. 6D). We next calculated the wound healing rates for each wound by dividing the total area healed (the initial wound area subtracted the final wound) by the number of days that the wound had been monitored, as described previously [27]. Healing rates for control wound group, wound received CHC hydrogel along or iPSC/CHC hydrogel were listed in Table 2. These in vivo evidences demonstrated that iPSC treatment in conjunction with CHC hydrogel application effectively promoted

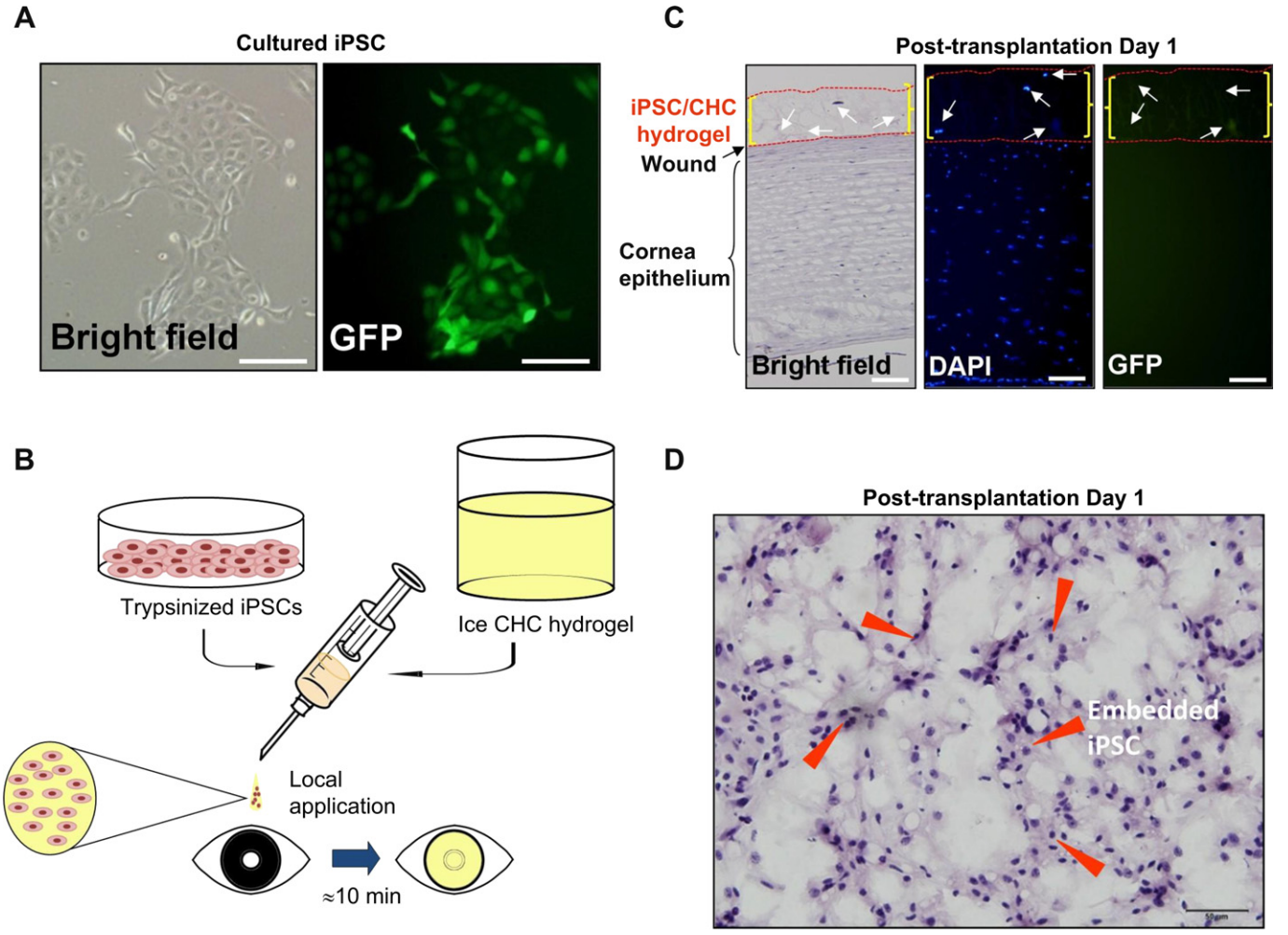

Fig. 5. Evaluation of the utility of the iPSC/CHC hydrogel combination in ex vivo transplantation. (A) An in vivo culture of a keratocyte-reprogrammed iPSC monolayer. Scale bar = 40 μm. (B) Procedure for iPSC/CHC hydrogel application onto the corneal wound. (C) Longitudinal sections of the eye indicating that the iPSC/CHC hydrogel mixture formed a smooth bio-scaffold layer on the surface of the corneal wound. Left: bright field; middle: viable cells detected using DAPI fluorescence staining; right: GFP-expressing iPSCs detected using GFP imaging. Scale bar = 200 μm. (D) Histological analysis and H & E staining showing the nanocapsule microstructure of the CHC hydrogel in which iPSCs were intercalated. Scale bar = 50 μm.

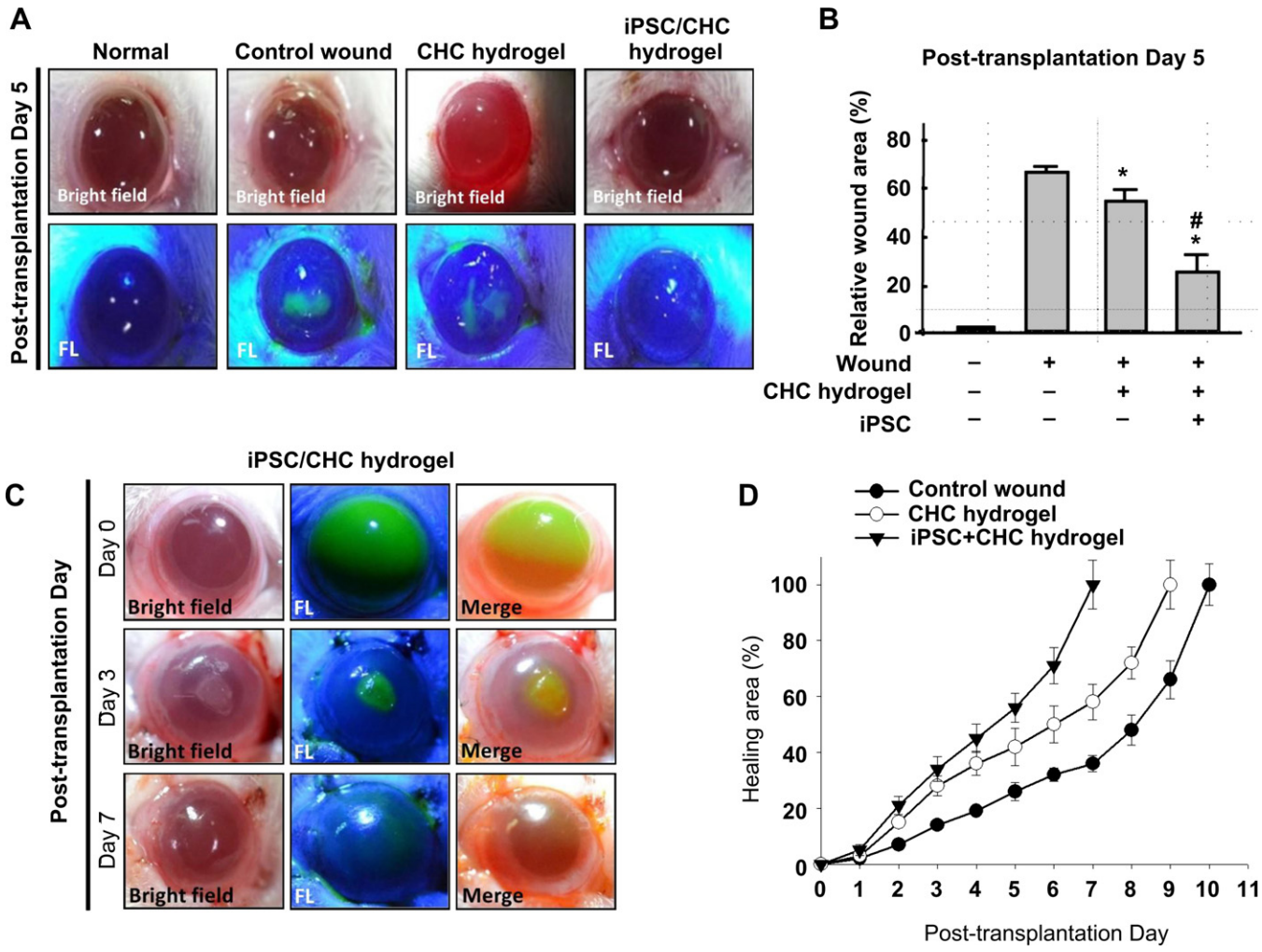

Fig. 6. Effects of iPSC/CHC hydrogel treatment on wound healing in abrasion-induced cornea injuries (A) Effects of the CHC hydrogel, iPSCs alone, or the combination of iPSCs and the CHC hydrogel on wound healing at day 5 after corneal abrasion. (B) Corneal wound area stained with fluorescent dye and quantified under UV light (lower). (C) Effects of the combined iPSC/CHC hydrogel treatment on wound healing at days 0, 3, and 7 post-injury. (D) Comparison of wound healing rate in groups including control wound, CHC hydrogel, iPSC/CHC hydrogel, along the post-transplantation days. Corneal wound area stained with fluorescent dye and quantified under UV light. The data shown here are the mean ± SD from three independent experiments. In panel B, $^{*}P < 0.05$ vs. wound. In panel D, $^{*}P < 0.05$ vs. iPSCs or CHC hydrogel alone.

corneal wound repair with accelerated wound healing rate in corneas injured by abrasion.

3.6. Epithelium restoration and decreased oxidative stress

The dynamic equilibrium of the corneal epithelium is regulated by limbal stem cells (LSCs). Dysfunctional LSCs create a pathological state known as LSC deficiency. To investigate whether the iPSC/CHC hydrogel combined treatment promoted corneal reconstruction, we induced severe corneal damage through abrasions accompanied by alkaline burns and evaluated the therapeutic efficacy of the iPSC/CHC hydrogel combination in repairing this damage (Fig. 7A). At day 7 and 14 after alkaline insult, Gross findings and GPF imaging revealed that severe corneal damage remained observable (Fig. 7A–C). Compared with the control wound group, the application of CHC hydrogel alone had a mild therapeutic effect, promoting corneal wound healing. Similar to the experiment involving corneal wounds induced only by abrasion (Fig. 6), after alkaline injury, the combination of the CHC hydrogel and iPSCs resulted in the greatest enhancement of corneal wound healing (Fig. 7B and C), leading to nearly complete corneal wound healing at day 14 (Fig. 7C). We traced the GFP signal of transplanted iPSCs and measured the thickness of the corneal epithelium in the alkaline burn corneal damage model. Notably, the epithelial thickness increased progressively following application of the iPSC/CHC hydrogel mixture and had recovered to a nearly normal thickness at post-injury day 14 (Fig. 8A upper and B). Meanwhile, the rough surface of the corneal epithelium was completely replaced by intact epithelium (Fig. 8A upper and the inset). GFP imaging revealed that transplanted iPSCs aggregated maximally on the surface of the corneal wound at day 7, whereas the GFP signal gradually declined through day 12 after iPSC transplantation, suggesting that the transplanted iPSCs were

Table 2
Wound healing rates in abrasion-injured cornea with indicated treatment.

Group	*n*	Growth/day (mean ± SD, percent wound healing /day)
Control wound	6	10 ± 1.25
Wound + CHC hydrogel	6	11.11 ± 1.45*
Wound + CHC hydrogel/iPSC	6	14.29 ± 1.47*, #

Results were expressed as mean ± SD (percent wound healing/day) from six experiments. $^{*}P < 0.05$ vs. control wound; $^{\#}P < 0.05$ vs. Wound + CHC hydrogel.

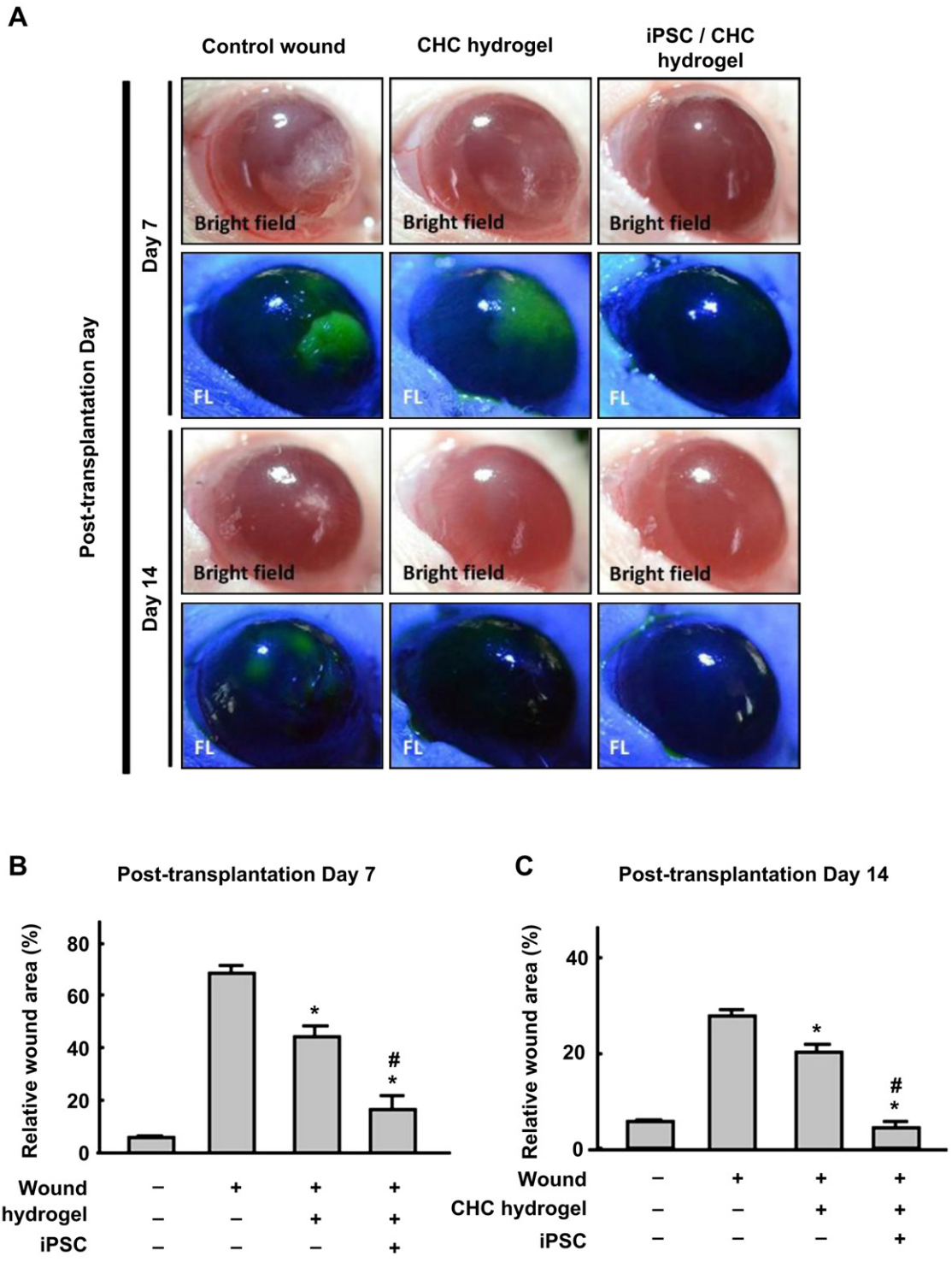

Fig. 7. Effects of the iPSC/CHC hydrogel combination treatment on wound healing in a chemical injury corneal damage model (A) Effects of the CHC hydrogel alone, iPSCs alone, or the iPSC/CHC hydrogel combination treatment on wound healing at days 7 (upper) and 14 (lower) after corneal abrasion and alkaline burning. Note that the corneal epithelial and stroma layers of the control damage group were damaged by the chemical insult. Corneal wound area stained with fluorescent dye and quantified under UV light at days (B) 7 and (C) 14 post-injury. The data shown here are the mean ± SD of three independent experiments. In panels B and C, $^{*}P < 0.05$ vs. control wound, $\#P < 0.05$ vs. CHC hydrogel only.

almost completely replaced by newly migratory epithelial cells (Fig. 8A middle). Remarkably, in the recipients of human keratocyte-reprogrammed iPSCs, neither gross necropsy findings nor histological examination revealed tumor-like structures in the cornea or other orbital areas (Table 3) in an extended follow-up study for eight weeks after application of the iPSC/CHC hydrogel combination. Previous evidences have demonstrated that iPSCs exhibited reactive oxygen species (ROS) defense mechanism and ROS scavenging activity [14,28]. Our data further showed that inducible NO synthetase (iNOS) was evident in control corneal wound induced by abrasions accompanied by alkaline burns. CHC hydrogel alone mildly suppressed iNOS expression, and the

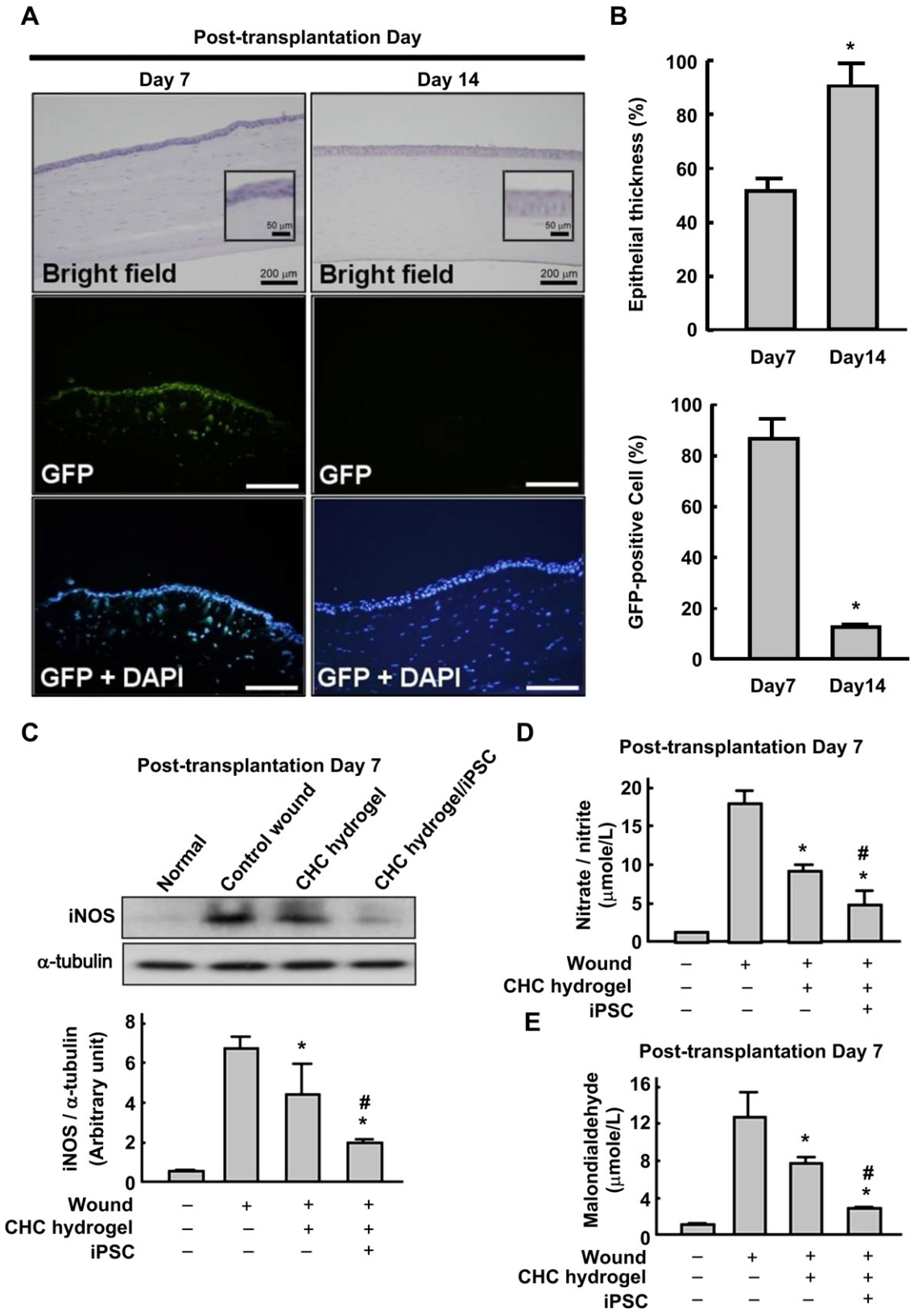

Fig. 8. Effects of iPSC engraftment on corneal epithelial thickness and endogenous epithelial cell migration in a chemical injury model of corneal damage. (A) Effects of the iPSC/CHC hydrogel combination treatment on endogenous epithelial cell migration at days 7 and 14 after corneal abrasion and alkaline insult. Upper: bright field; middle: GFP-expressing iPSCs detected via GFP imaging; lower: viable cells detected using a fluorescent DAPI stain. Scale bar = 200 μm. A higher magnification image illustrating the reconstruction of epithelium surface was shown in the insets. Scale bar = 50 μm. (B) Quantification of cornea epithelial thickness at days 7 and 14 after the alkaline insult (upper). Quantification of GFP-positive cell numbers at days 7 and 14 after the alkaline insult (lower). (C) Western blot showed that iPSC/CHC hydrogel downregulates inducible NO synthetase (iNOS) expression in damaged cornea. Changes in (D) nitrate/nitrite and (E) malondialdehyde content in damaged cornea treated with CHC hydrogel alone or CHC hydrogel/iPSCs. The data shown here are the mean ± SD of three independent experiments. In panel B, $^{*}P < 0.05$ vs. day 7. In panels C, D and E, $^{*}P < 0.05$ vs. control wound, $\#P < 0.05$ vs. CHC hydrogel only.

Table 3
Incidence of tumor formation in recipients of human corneal keratocyte-reprogrammed iPSCs eight weeks after iPSC/CHC hydrogel treatment.

Follow-up time	2 wks	4 wks	6 wks	8 wks
Cornea	0/6	0/6	0/6	0/6
Orbital area	0/6	0/6	0/6	0/6

combined treatment of iPSC/CHC hydrogel almost abolished the iNOS expression (Fig. 8C). There was a significant increase in nitrate/nitrite and malondialdehyde levels in control wound cornea compared to normal cornea (Fig. 8D and E). These increases were significantly reduced by the addition of CHC hydrogel alone and were maximally suppressed by the combined treatment of iPSC/CHC hydrogel (Fig. 8D and E). Taken together, the ROS scavenging ability of iPSC and the increase in corneal epithelium thickness following the iPSC/CHC hydrogel combination treatment demonstrated that the iPSCs enhanced corneal wound healing by suppressing ROS generation and stimulating tissue remodeling, probably via rescuing the LSC deficiency.

4. Discussion

Unlike the permanent visual loss that results from retinal disorders and glaucoma, the majority of corneal injury-related vision losses could be reversed by corneal transplantation or stem cell therapy. The generation of iPSCs is an innovative technology that reprograms adult somatic cells into ESC-like cells through exogenous expression of Yamanaka factors. Nevertheless, information about the potential of corneal keratocyte-reprogrammed iPSCs to modulate wound healing and the ability of endogenous stem cells to effect corneal reconstruction is still lacking. The first aim of this study was to address whether adult cornea-derived somatic cells can be employed to generate human iPSCs. Using the four-gene delivery method (Oct4/Sox2/Klf4/c-Myc), we successfully created iPSCs by de-differentiating corneal keratocytes isolated from surgical residues of donor cornea tissues after transplantation. Under a serum-free and feeder-free cultured system, these iPSCs remained stable through 30 passages, while retaining ESC-like pluripotency. The EBs derived from these keratocyte-reprogrammed iPSCs could be differentiated into both neuroectodermal lineage neuron-like cells and mesodermal lineages. Recent studies showed that de-differentiation of rabbit corneal epithelial cells to a less terminally differentiated stage could be induced with ESC extracts [29], thus raising the possibility that these human cornea-derived iPSCs could be used as an unlimited stem cell source for cell differentiation or tissue engineering therapies in corneal or other ophthalmic diseases. We further investigated the potential of human keratocyte-reprogrammed iPSCs to be used as bioengineered substitutes in corneal repair. Our data confirmed that these human keratocyte-reprogrammed iPSCs, combined with CHC hydrogel, can be used as a rapid delivery system for efficient enhancement of corneal healing in a corneal abrasion model. Moreover, in an in vivo mouse model of chemical injury, the combination of human keratocyte-reprogrammed iPSCs and CHC hydrogel also significantly accelerated corneal wound healing. No incidence of tumorigenesis was detected in an extended follow-up study after application of the iPSCs/CHC hydrogel combination. Thus, our data demonstrate that iPSCs play a crucial role in the process of corneal wound healing and that CHC nanogel may provide a safe delivery system for stem cell therapies for severe corneal injuries.

Using immortalized cell lines, Griffith et al. constructed artificial human cornea equivalents comprised of an epithelium, stroma, and endothelium that mimicked human cornea functionality [30]. In addition, multiple approaches have been developed to reproduce the optical properties of the cornea, including the use of self-assembled corneal substitutes involving dermal or corneal fibroblasts [31–33], acellular tissue-engineered scaffolds designed to induce endogenous precursor cells to effect repair [34–36], and tissue-engineered scaffolds for stem cell or progenitor cell delivery [37,38]. A thermo-reversible hydrogel has been developed and used as a biosynthetic bandage for corneal wound repair [39]. Builles et al. reported that magnetically oriented orthogonal collagen scaffolds, human limbal stem cell (LSC)-derived epithelial cells and primary keratocytes can be used to engineer a human hemi-cornea (stroma and epithelium) [40]. In this study, we used keratocyte-reprogrammed iPSCs as bioengineered corneal substitutes and studied the bioavailability of CHC hydrogel for creating an iPSC niche and iPSC transplantation. Indeed, our data demonstrated that these hydrogels exhibited several favorable characteristics, including injectability, time-saving properties, thermosensitivity, biocompatibility, and a lack of amniotic membrane-based transplantation (AMT)-related biohazards. It has been shown that hyaluronic acid modulates CD44 to regulate the differentiation of bone marrow progenitor-derived cells into fibroblast-like cells [41]. In addition, low-molecular weight hyaluronic acid substrates were reported to be effective in maintaining the viability and pluripotency properties of murine ESCs [42]. Similarly, our data indicate that CHC nanogel can maintain cell viability and the expression of embryonic stem-like factors in corneal keratocyte-reprogrammed iPSCs when cultured in vitro with stem cell medium. It is worthwhile to note that CHC nanoscale hydrogel could also promote the proliferation of CD44+ subset in cultured iPSCs. Taken together, our data suggested that the CHC nanoscale hydrogel enhances the functional potential of iPSCs to maintain their self-renewal ability and an ESC-like gene expression pattern. To further investigate the development of bioactive and biocompatible scaffolds for the reconstruction and regeneration of the cornea and other tissues, it will be critical to explore whether specific modifications of CHC or other hyaluronic acid-based nanomaterials can regulate stem cell renewal or facilitate lineage-specific differentiation.

Cornea is known to ensure the normal vision by refracting light onto the lens and retina. The epithelial tight functional integrity of cornea is essential for the corneal optical properties when the corneal epithelium undergoes continuous renewal. As the superficial differentiated cells are lost by desquamation, these cells are substituted by the underlying proliferating basal cell layer [43]. Limbal stem cells (LSCs) can maintain the dynamic proliferation of corneal epithelial cells, reinforce the physiological functioning of the ocular surface, and play an essential role in repairing human corneal injuries via epithelial reproduction. LSC deficiency manifests as a severe disease characterized by the inability to replenish the corneal epithelium, and this deficiency may eventually result in blindness [44]. In the pursuit of a clinical solution to LSC deficiency, it has been demonstrated that human limbal epithelial stem cells can be expanded ex vivo on amniotic membrane cultures [45]. In this study, we demonstrated that human corneal keratocyte-reprogrammed iPSCs combined with CHC nanogel can efficiently facilitate corneal reconstruction in an alkaline-induced model of corneal injury and LSC deficiency. In addition, CHC nanogel can facilitate the engraftment of iPSCs into chemically injured corneal tissues, including the corneal epithelial and stromal layers (Fig. 7A). It is well known that the reconstruction of the corneal microenvironment may enable the remnant LSCs to resume their function in maintaining corneal transparency [46]. We also found that keratocyte-reprogrammed iPSCs seeded into CHC hydrogel can increase the epithelial cell growth in damaged corneas and promptly recover the thickness of corneal epithelium. Indeed, these engrafted iPSCs preserved the integrity of the ocular surface and

may also provide a stem cell niche to promote endogenous LSC proliferation. Remarkably, after application of iPSC/CHC hydrogel combination, no incidence of tumor formation was observed within eight weeks (Table 3) and neither GFP-labeled cells nor undifferentiated iPSCs were detectable in the reconstructed cornea (Fig. 8A). Considering that complete turnover of corneal epithelial cells occurs in about 7–10 days [47,48], it is plausible to speculate that transplanted iPSCs were lost and replaced by underlying proliferating cells during the renewal process in reconstructed corneal epithelium. Further in vivo kinetic study of engrafted iPSCs in corneal epithelium turnover will be necessary to validate such interpretation.

Along with previous observations that iPSCs are able to defend antioxidants by maintaining low levels of ROS [28] and to suppress oxidative stress in vivo [14], we also found that keratocyte-reprogrammed iPSCs exhibited antioxidant activity that suppressed nitrate/nitrite and malondialdehyde levels at the damage sites of cornea (Fig. 8). Therefore, iPSCs can play an important role in corneal wound healing by recruiting endogenous stem cells and reconstructing the corneal microenvironment niche. In the future, cell therapy using non-viral vectors or transgene-free iPSCs may improve corneal injury prognoses and provide an alternative adjuvant treatment for severe corneal injuries.

5. Conclusions

In the present report, we provided an injectable, thermosensitive platform for delivering stem cell-based grafts that not only represents an ex vivo expansion of useful corneal reconstruction strategies but also offers an important opportunity to improve wound healing therapeutics in cell-based regeneration therapies for ocular diseases. In addition, with this iPSC-based technology, surgical residues which are usually regarded as medical waste, can be employed as an alternative source of pluripotent stem cells for personalized medicine.

Acknowledgements

This study was assisted in part by the Center for Stem Cell Research, and Division of Experimental Surgery of the Department of Surgery Taipei Veterans General Hospital. This study was funded by NSC-(100-2120-M-002-011, 100-2325-B-010-010, 100-2321-B-010-020), the Joint Projects of VGHUST & UTVGH (VN100-03 & VN101-06). Taipei Veterans General Hospital (Stem Cell Project E99-101), Yen-Tjing-Ling Medical Foundation (CI-99/100), The Department of Health Cancer Center Research of Excellence (DOH101-TD-C-111-007), The Genomic Center Project of National Yang-Ming University (Ministry of Education, Aim for the Top University Plan).

Appendix A. Supplementary material

Supplementary material associated with this article can be found, in the online version, at http://dx.doi.org/10.1016/j.biomaterials.2012.07.029.

References

[1] Cotsarelis G, Cheng SZ, Dong G, Sun TT, Lavker RM. Existence of slow-cycling limbal epithelial basal cells that can be preferentially stimulated to proliferate: implications on epithelial stem cells. Cell 1989;57(2):201–9.
[2] Davanger M, Evensen A. Role of the pericorneal papillary structure in renewal of corneal epithelium. Nature 1971;229(5286):560–1.
[3] Zhao X, Das AV, Thoreson WB, James J, Wattnem TE, Rodriguez-Sierra J, et al. Adult corneal limbal epithelium: a model for studying neural potential of non-neural stem cells/progenitors. Dev Biol 2002;250(2):317–31.
[4] Grueterich M, Tseng SC. Human limbal progenitor cells expanded on intact amniotic membrane ex vivo. Arch Ophthalmol 2002;120(6):783–90.
[5] Arsenijevic Y, Taverney N, Kostic C, Tekaya M, Riva F, Zografos L, et al. Non-neural regions of the adult human eye: a potential source of neurons? Invest Ophthalmol Vis Sci 2003;44(2):799–807.
[6] Tsai RJ, Li LM, Chen JK. Reconstruction of damaged corneas by transplantation of autologous limbal epithelial cells. N Engl J Med 2000;343(2):86–93.
[7] Srinivasan R, SS T, Gupta A, Kaliaperumal S. Hypopyon iritis after primary fresh amniotic membrane transplantation. Cornea 2007;26(10):1275–6.
[8] Das S, Ramamurthy B, Sangwan VS. Fungal keratitis following amniotic membrane transplantation. Int Ophthalmol 2009;29(1):49–51.
[9] Marangon FB, Alfonso EC, Miller D, Remonda NM, Muallem MS, Tseng SC. Incidence of microbial infection after amniotic membrane transplantation. Cornea 2004;23(3):264–9.
[10] Robinton DA, Daley GQ. The promise of induced pluripotent stem cells in research and therapy. Nature 2012;481(7381):295–305.
[11] Park IH, Zhao R, West JA, Yabuuchi A, Huo H, Ince TA, et al. Reprogramming of human somatic cells to pluripotency with defined factors. Nature 2008;451(7175):141–6.
[12] Okita K, Ichisaka T, Yamanaka S. Generation of germline-competent induced pluripotent stem cells. Nature 2007;448(7151):313–7.
[13] Yu J, Vodyanik MA, Smuga-Otto K, Antosiewicz-Bourget J, Frane JL, Tian S, et al. Induced pluripotent stem cell lines derived from human somatic cells. Science 2007;318(5858):1917–20.
[14] Li HY, Chien Y, Chen YJ, Chen SF, Chang YL, Chiang CH, et al. Reprogramming induced pluripotent stem cells in the absence of c-Myc for differentiation into hepatocyte-like cells. Biomaterials 2011;32(26):5994–6005.
[15] Yang KY, Shih HC, How CK, Chen CY, Hsu HS, Yang CW, et al. IV delivery of induced pluripotent stem cells attenuates endotoxin-induced acute lung injury in mice. Chest 2011;140(5):1243–53.
[16] Chen SJ, Chang CM, Tsai SK, Chang YL, Chou SJ, Huang SS, et al. Functional improvement of focal cerebral ischemia injury by subdural transplantation of induced pluripotent stem cells with fibrin glue. Stem Cells Dev 2010;19(11):1757–67.
[17] Zhou L, Wang W, Liu Y, Fernandez de Castro J, Ezashi T, Telugu BP, et al. Differentiation of induced pluripotent stem cells of swine into rod photoreceptors and their integration into the retina. Stem Cells 2011;29(6):972–80.
[18] Schwartz SD, Hubschman JP, Heilwell G, Franco-Cardenas V, Pan CK, Ostrick RM, et al. Embryonic stem cell trials for macular degeneration: a preliminary report. Lancet 2012;379(9817):713–20.
[19] Lin T, Ambasudhan R, Yuan X, Li W, Hilcove S, Abujarour R, et al. A chemical platform for improved induction of human iPSCs. Nat Methods 2009;6(11):805–8.
[20] Deb-Rinker P, Ly D, Jezierski A, Sikorska M, Walker PR. Sequential DNA methylation of the Nanog and Oct-4 upstream regions in human NT2 cells during neuronal differentiation. J Biol Chem 2005;280(8):6257–60.
[21] Huangfu D, Osafune K, Maehr R, Guo W, Eijkelenboom A, Chen S, et al. Induction of pluripotent stem cells from primary human fibroblasts with only Oct4 and Sox2. Nat Biotechnol 2008;26(11):1269–75.
[22] Chen YC, Hsu HS, Chen YW, Tsai TH, How CK, Wang CY, et al. Oct-4 expression maintained cancer stem-like properties in lung cancer-derived CD133-positive cells. PLoS One 2008;3(7):e2637.
[23] Liu TY, Chen SY, Lin YL, Liu DM. Synthesis and characterization of amphiphatic carboxymethyl-hexanoyl chitosan hydrogel: water-retention ability and drug encapsulation. Langmuir 2006;22(23):9740–5.
[24] Ling S, Qi C, Li W, Xu J, Kuang W. Crucial role of corneal lymphangiogenesis for allograft rejection in alkali-burned cornea bed. Clin Exp Ophthalmol 2009;37(9):874–83.
[25] Liu KH, Chen BR, Chen SY, Liu DM. Self-assembly behavior and doxorubicin-loading capacity of acylated carboxymethyl chitosans. J Phys Chem B 2009;113(35):11800–7.
[26] Svee K, White J, Vaillant P, Jessurun J, Roongta U, Krumwiede M, et al. Acute lung injury fibroblast migration and invasion of a fibrin matrix is mediated by CD44. J Clin Invest 1996;98(8):1713–27.
[27] Gorin DR, Cordts PR, LaMorte WW, Manzoian JO. The influence of wound geometry on the measurement of wound healing rates in clinical trials. J Vasc Surg 1996;23(3):524–8.
[28] Armstrong L, Tilgner K, Saretzki G, Atkinson SP, Stojkovic M, Moreno R, et al. Human induced pluripotent stem cell lines show stress defense mechanisms and mitochondrial regulation similar to those of human embryonic stem cells. Stem Cells 2010;28(4):661–73.
[29] Zhan W, Liu Z, Liu Y, Ke Q, Ding Y, Lu X, et al. Modulation of rabbit corneal epithelial cells fate using embryonic stem cell extract. Mol Vis 2010;16:1154–61.
[30] Griffith M, Osborne R, Munger R, Xiong X, Doillon CJ, Laycock NL, et al. Functional human corneal equivalents constructed from cell lines. Science 1999;286(5447):2169–72.
[31] Gonzalez-Andrades M, de la Cruz Cardona J, Ionescu AM, Campos A, Del Mar Perez M, Alaminos M. Generation of bioengineered corneas with decellularized xenografts and human keratocytes. Invest Ophthalmol Vis Sci 2011;52(1):215–22.
[32] Guo X, Hutcheon AE, Melotti SA, Zieske JD, Trinkaus-Randall V, Ruberti JW. Morphologic characterization of organized extracellular matrix deposition by ascorbic acid-stimulated human corneal fibroblasts. Invest Ophthalmol Vis Sci 2007;48(9):4050–60.

[33] Du Y, Sundarraj N, Funderburgh ML, Harvey SA, Birk DE, Funderburgh JL. Secretion and organization of a cornea-like tissue in vitro by stem cells from human corneal stroma. Invest Ophthalmol Vis Sci 2007;48(11):5038–45.
[34] Crabb RA, Chau EP, Evans MC, Barocas VH, Hubel A. Biomechanical and microstructural characteristics of a collagen film-based corneal stroma equivalent. Tissue Eng 2006;12(6):1565–75.
[35] Merrett K, Fagerholm P, McLaughlin CR, Dravida S, Lagali N, Shinozaki N, et al. Tissue-engineered recombinant human collagen-based corneal substitutes for implantation: performance of type I versus type III collagen. Invest Ophthalmol Vis Sci 2008;49(9):3887–94.
[36] Liu W, Merrett K, Griffith M, Fagerholm P, Dravida S, Heyne B, et al. Recombinant human collagen for tissue engineered corneal substitutes. Biomaterials 2008;29(9):1147–58.
[37] Nakamura T, Inatomi T, Sotozono C, Ang LP, Koizumi N, Yokoi N, et al. Transplantation of autologous serum-derived cultivated corneal epithelial equivalents for the treatment of severe ocular surface disease. Ophthalmology 2006;113(10):1765–72.
[38] Rama P, Bonini S, Lambiase A, Golisano O, Paterna P, De Luca M, et al. Autologous fibrin-cultured limbal stem cells permanently restore the corneal surface of patients with total limbal stem cell deficiency. Transplantation 2001;72(9):1478–85.
[39] Pratoomsoot C, Tanioka H, Hori K, Kawasaki S, Kinoshita S, Tighe PJ, et al. A thermoreversible hydrogel as a biosynthetic bandage for corneal wound repair. Biomaterials 2008;29(3):272–81.
[40] Builles N, Janin-Manificat H, Malbouyres M, Justin V, Rovere MR, Pellegrini G, et al. Use of magnetically oriented orthogonal collagen scaffolds for hemicorneal reconstruction and regeneration. Biomaterials 2010;31(32):8313–22.
[41] Maharjan AS, Pilling D, Gomer RH. High and low molecular weight hyaluronic acid differentially regulate human fibrocyte differentiation. PLoS One 2011; 6(10):e26078.
[42] Joddar B, Kitajima T, Ito Y. The effects of covalently immobilized hyaluronic acid substrates on the adhesion, expansion, and differentiation of embryonic stem cells for in vitro tissue engineering. Biomaterials 2011;32(33):8404–15.
[43] Lu L, Reinach PS, Kao WW. Corneal epithelial wound healing. Exp Biol Med (Maywood) 2001;226(7):653–64.
[44] Shortt AJ, Secker GA, Notara MD, Limb GA, Khaw PT, Tuft SJ, et al. Transplantation of ex vivo cultured limbal epithelial stem cells: a review of techniques and clinical results. Surv Ophthalmol 2007;52(5):483–502.
[45] Tseng SC, Meller D, Anderson DF, Touhami A, Pires RT, Gruterich M, et al. Ex vivo preservation and expansion of human limbal epithelial stem cells on amniotic membrane for treating corneal diseases with total limbal stem cell deficiency. Adv Exp Med Biol 2002;506(Pt B):1323–34.
[46] Ordonez P, Di Girolamo N. Limbal epithelial stem cells: role of the niche microenvironment. Stem Cells 2012;30(2):100–7.
[47] Hanna C, Bicknell DS, O'Brien JE. Cell turnover in the adult human eye. Arch Ophthalmol 1961;65:695–8.
[48] Buck RC. Measurement of centripetal migration of normal corneal epithelial cells in the mouse. Invest Ophthalmol Vis Sci 1985;26(9):1296–9.